Energy structure of $KTaO_3$ and $KTaO_3$:Li

I. I. Tupitsyn
St.-Petersburg State University, Petergoff, Uljanovskaya 1, 190804 St. Petersburg, Russia

A. Deineka, V. A. Trepakov,* and L. Jastrabik
Institute of Physics, Academy of Sciences of the Czech Republic, Na Slovance 2, 182 21 Prague 8, Czech Republic

S. E. Kapphan
FB Physik, Osnabrück University, D-49069 Osnabrück, Germany

(Received 3 February 2000; revised manuscript received 14 May 2001; published 17 October 2001)

Ab initio energy structure calculations of pure $KTaO_3$ (KTO) and $KTaO_3$ doped with Li (KTL) were performed using the CASTEP code [M.C. Payne, M.P. Teter, D.C. Alan, T.A. Arias, and J.D. Joannopoulos, Rev. Mod. Phys. **64**, 1045 (1992)] based on the density functional theory (DFT) and the intermediate neglect of the differential overlap INDO method. The optimized lattice parameters of perfect KTO calculated in this work are in a good agreement with the available experimental data. The population analysis shows that KTO has a mixed ionic-covalent type of bonds. DFT calculations for the KTL have been performed for a $2\times2\times2$ supercell of KTO with one Li^+ substituting K^+. The Li^+ off-center ion and nearest oxygen displacements are defined. It was shown that oxygen displacements around Li^+ off-center ions lead to the production of two local states in the bandgap at 60 meV and 90 meV from the top of the valence band, which in all probability play an important role in the photostimulated processes.

DOI: 10.1103/PhysRevB.64.195111 PACS number(s): 71.20.-b

I. INTRODUCTION

The most popular model object of ABO_3 perovskite-like ferroelectrics, an incipient ferroelectric potassium tantalate is characterized by a high value of the dielectric constant increasing with the temperature cool down. At lowest temperatures KTO practically loses stability to polarization distortions, but remains paraelectric cubic due to quantum fluctuations. However, because of inherent instability, even low level of appropriate doping can induce phase transition with strong changes in physical properties. Doping with Li, which substitutes K in the *A* position of the ABO_3 perovskite-type lattice and forms Li^+ off-center ions with large (1.2 Å) displacements along $\langle 100\rangle$ direction, is one of the most interesting and actively studied cases.[1–3] Here depending on the Li content, various phases from dipole glass-like to ferroeletric ones can be realized. Because of the large displacement of the Li^+ ions it is reasonable to suspect the corresponding changes in its electronic structure and ''electronic related'' properties of the KTO. Indeed, as it was shown in Ref. 4, Li doping of KTO leads to the appearance of the large photoconductivity at low temperatures, which increases sharply at the dipole-glass freezing temperature T_f. This photoconductivity enhancement at T_f, was assigned to the presence of hole traps in KTL at lower temperatures, which hinders the recombination of photocarriers. The authors of Ref. 4 suggested that these shallow traps are originating from the perturbation of O^{2-} levels due to oxygen ion displacements under the influence of the Li^+ off-center ions. As a result, Li^+ off-center freezing at T_f is accompanied by the enhancement of the photoconductivity in the dipole glass transition region. Similar effects for impurities substituting the *A*-host ions have been found also in SrTiO3:Ca (Ref. 5), where a giant photoconductivity response was observed at lowest temperatures. It seems, that enhancement of photoconductivity at low temperatures in ABO_3 perovskite-type oxides with freezing of impurity off centers in *A* position is rather common phenomena.

There are strong experimental evidences that Li doping and corresponding appearance of shallow levels lead to the increase of the photoluminescence intensity, the appearance of thermostimulation current and long time photoluminescence, and photocurrent relaxations in KTL.[6–8] These phenomena together with scar or contradictory data of the KTO band structure details (see, e.g., Refs. 9–11, and references therein) and the absence of calculations of Li doping effect in energy structure, encouraged us to perform first energy structure calculations for KTL with additional comparative calculations of the KTO energy structure. Such studies give new insight to the structure of impurity centers, doping effects in the energy structure, photoinduced properties. Furthermore, they are useful for the development of the microscopic theory of impurity induced structural transformations in KTO and related ionic-covalent materials. We employed the density functional theory (DFT) in the local density approximation (LDA) and INDO methods and compared the results with previous work.[9,10] The optimization of the lattice parameters of KTO and KTL have been performed in the frame of DFT method. A periodic defect model with a $2\times2\times2$ supercell for the total energy calculations of KTL was used. Since the size of the supercell was not large enough to define the nature of the local defect states in the gap, the simpler INDO method with $4\times4\times4$ supercell was employed to calculate one-electron energies and wave functions of the defect states with the fixed geometry. The parameters of the INDO method were fitted to reproduce the DFT band structure of pure KTO.

II. METHOD

Two methods were used for the KTO and KTL band structure calculations. The first one was the DFT method. This method is based on the density functional theory and concrete calculations were made with the CASTEP code, which uses a plane wave basis set for the valence electrons. Here a pseudopotential theory was used in order to include the effect of the core states. The number of plane waves included into the basis was determined by a cutoff energy E_c. Test calculations were performed with $E_c = 560$, 600, and 650 eV . Convergence of calculation parameters for perfect KTO (total energy, widths of conduction and valence bands etc.) was reached for a magnitude of $E_c = 600$ eV.

Taking into account the core states, atomic pseudopotentials were added in our calculations. Pseudopotentials of K, Ta, O, and Li were made beforehand by using an optimized version of Kerker's scheme.[12] These pseudopotentials are semilocal norm-conserving effective core potentials. The optimized Kerker's scheme allows the making of ultrasoft potentials, in which the Fourier components converge very quickly with the increasing of the vector of the reciprocal lattice. Because of computational reasons, the semilocal pseudopotentials were replaced by separable potentials written in Kleinman-Bylander form.[13] In order to test the quality of the Ta pseudopotential obtained, a number of nonempirical electronic structure calculations were performed for the TaO molecule using the CASTEP codes. A large unit cubic cell was employed to eliminate interaction between the molecules in different cells. Various values were used for the cutoff energy which determines the number of plane wave basis states. Inspection of the results obtained shows that the cutoff energy of 650 eV is large enough. The calculated equilibrium inter-atomic distance (1.767 Å) is in good agreement with the experimental value (1.749 Å), the difference being less than 0.02 Å for the TaO molecule. The small deviation may be caused by the fact that TaO is a system with open shells. The ground state of this molecule is $^2\Delta$. It is a well-known fact that the LDA approximation is not very good for open-shell systems.

The second method was the INDO method (a semiempirical variant of the unrestricted Hartree-Fock method). The linear combination of atomic orbitals (LCAO) in the basis of double-ζ[14] Slater type orbitals (STO) is used here in this method. The double-ζ basis was used before to perform electronic structure calculations of $3d$-oxide crystals (see, for example, Ref. 15). The basis of the method is the neglect of differential overlap (NDO) that means the neglect of all two-electron multicentered integrals with multiplication of functions localized in different centers. In our calculations all one-centered integrals (Coulomb-type F_k and exchange-type G_k), which provide atomic multiplet structure, were calculated *ab initio* in the STO basis. As fit parameters were taken $U_{\mu\mu}$ (core potential parameter), $\gamma_{aa} = F_0$ (effective Coulomb repulsion of two electrons on one center), and β (resonant integral). For describing the Coulomb interaction γ_{AB} of electrons of different atoms we used the modified Ohno-Klopman equation,[16] which differs from the standard one by the correct asymptotic approximations for high interatomic distances. The Ohno-Klopman equation was suggested for the molecular CNDO and INDO calcultions for not too high interatomic distances. In the infinite crystal the nonpoint part of the Ohno expression has a wrong $1/r^2$ asymptotic behavior which leads to unphysical divergencies in the Coulomb potential and Coloumb energy. To overcome this problem we did smooth the Ohno expression with point Coulomb $1/r$ asymptotic approximation for the distances larger than 7 a.u. This procedure is standard for the CNDO and INDO calculations of the crystals.

Hartree-Fock equations generally overestimate the gap (especially for the ionic crystals). There are two reasons of this overestimation. First there are intra-atomic correlations. The electron-electron one-center Coulomb repulsion is usually overestimated in the *ab initio* Hartree-Fock calculations.[15] In the INDO calculations the value of this repulsion γ_{aa} is close to the experimental parameter which is equal to the difference between the ionization potential of the atom and its electron affinity. The second reason are bulk polarization effects. We used the simple point lattice (Mott-Littleton) model in the INDO calculations to take into account the polarization effects induced by conduction band electron and valence band hole for the description of one-electron excitations.

The population analysis was carried out using the Kohn-Sham one-electron orbitals of the crystal (in the plane-wave basis set).[17] The Kohn-Sham orbitals ϕ_{Aa} of single atoms calculated with the same pseudopotential as in the crystal were employed. Here A denotes the atom (in the zero elementary cell) and a denotes the orbital. The atomic orbitals are not orthogonal. Using the Bloch sums $\phi_{Aa}(\mathbf{k})$ and the projecting technique,[17] the density matrix of the crystal $P_{Aa,Bb}(\mathbf{k})$ in the atomic orbital representation was calculated from the Kohn-Sham crystal orbitals. The standard transformation to the Löwdin orthonormal atomic basis

$$P^L(\mathbf{k}) = S^{1/2}(\mathbf{k}) P(\mathbf{k}) S^{1/2}(\mathbf{k}) \tag{1}$$

with the overlap matrix $S(\mathbf{k})$ was made first and then the Fourier transformation to the real space $P^L_{Aa,Bb}(\mathbf{R})$ density matrix was performed. Here the atom A is in the zero elementary cell and the atom B is in the elementary cell translated by the vector $\mathbf{R}$. Similarly, matrices

$$P^M(\mathbf{k}) = P(\mathbf{k}) S(\mathbf{k}) \tag{2}$$

and $P^M_{Aa,Bb}(\mathbf{R})$ for the Mulliken population analysis were calculated. With these matrices the charge on the atom A is defined as

$$Q^L_A = Z_A - \sum_{a \in A} P^L_{Aa,Aa}(0), \quad \text{Löwdin charge},$$

$$Q^M_A = Z_A - \sum_{a \in A} P^M_{Aa,Aa}(0), \quad \text{Mulliken charge}, \tag{3}$$

where Z_A is the nucleus charge. Another useful quantity are the Wiberg[18] and Mayer[19] indexes which are defined as

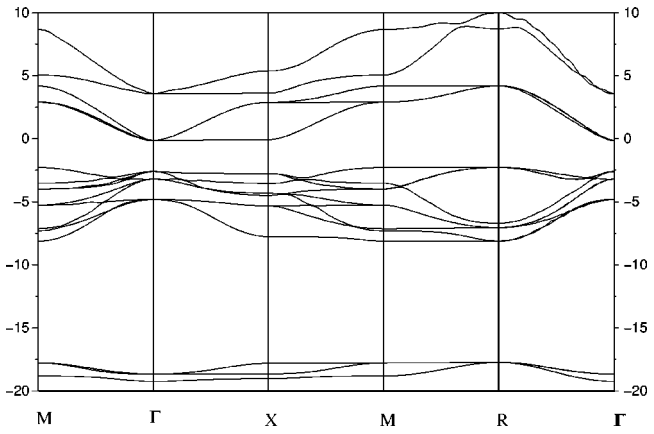

FIG. 1. Band structure of perfect $KTaO_3$ calculated by DFT method.

$$W_{AB}(\mathbf{R}) = \sum_{a \in A} \sum_{b \in B} |P^{L}_{Aa,Bb}(\mathbf{R})|^2. \quad (4)$$

The Wiberg index describes the bond order. For a pure covalent single bond $\psi = \phi_{Aa} + \phi_{Bb}$ the Wiberg index is equal to 1 and for pure double bonds it is equal to 2 and so on. The magnitudes of atomic covalence allow us to find the order of covalent and ionic bonds in the whole crystal.

For geometry optimization the calculation of perfect $KTaO_3$ using the DFT method was performed. The total energy was calculated as a function of the lattice constant for the cubic phase. The construction of a self-consistent electron density was performed for high-symmetry points of the Brillouin zone. The density obtained was used for calculations of the band structure and density of states (DOS) of the perfect KTO. In calculating DOS the zero energy level was chosen to be at the top of the valence band and the energy levels were broadened by the convolution with a Gauss function of 0.35 eV width. We used discrete Fourier transformation for the interpolation the energies $E(\vec{k})$ inside the BZ. The theoretical predictions are compared with experimental data reported for comparative studies of the optical absorption edge in KTO and KTL crystals.[20]

III. RESULTS AND DISCUSSIONS

Figure 1 shows the band structure of KTO, calculated by the DFT method. The value of the band gap obtained appears to be 2.1 eV, which is consistent with the theoretical estimations,[9,11] which gave also an underestimated band-gap magnitude as is typical in LDA and LMTO methods. However, this value is too small in respect to the values typically found in experiments of 3.79,[21] 3.3,[22] and 3.64 eV obtained in our optical absorption measurements for the direct optical gap of KTO.[20] The reason for such a disagreement is the well-known short coming of the local density approximation (LDA) for semiconductors and insulators. The top of the VB appears to be very flat and the bandgap of KTO and KTL is indirect with a minimum of the CB at the Γ point of the Brillouin zone (BZ), and a maximum of the VB at the M point. The CB is rather flat along the *X* direction, but the

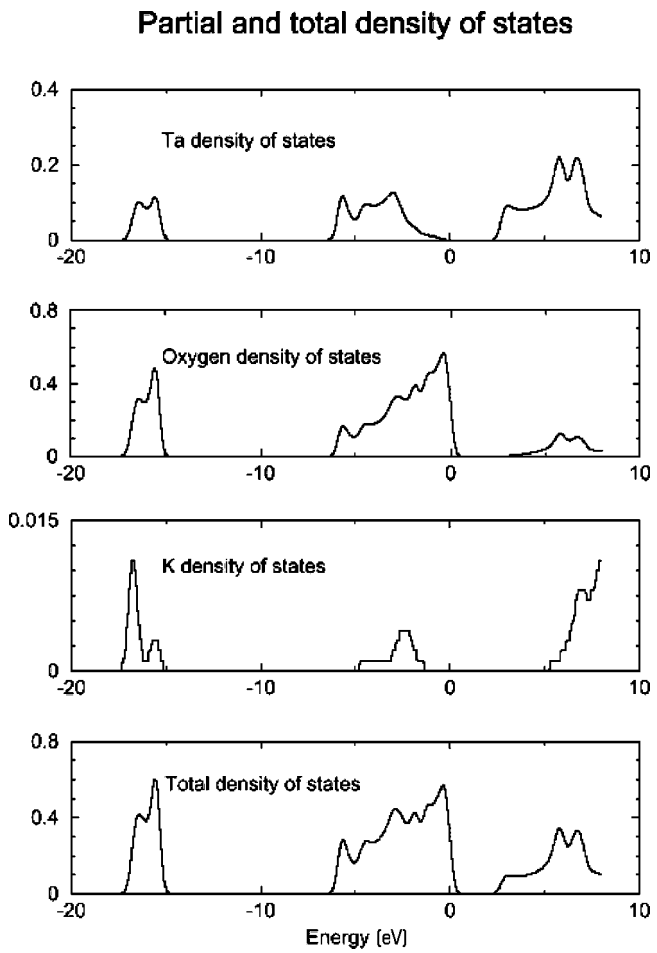

FIG. 2. Total and partial density of states of $KTaO_3$.

effective mass of the electrons is lower along the *R* direction. The top of the VB is formed by *p* states of oxygen and partially by *d* states of Ta, whereas the bottom of the conduction band is formed by *d* states of Ta as can be seen from Fig. 2, which presents the total and partial density of states. *S* states of K are located high up in the CB (much higher than the *d* states of Ta). The band structure obtained in our calculations appears rather similar to data of Refs. 9,10, but in some important details, the quantitative results appear to be quite different. So, we found that the bottom of the CB is much flatter along the M direction and we obtained the value of the effective mass of the electron in the lowest CB along the *M* directions $\sim 2.3 m_0$, that is larger than in Ref. 23. The shape of the top of the VB appears to be rather similar to Ref. 9 but more flat than in Ref. 10. And it is remarkable that in contrast to Ref. 10, our calculations predict that the maximum of the VB is located at the R point of the BZ. The same result was obtained in Ref. 9.

The calculated magnitudes of the Mulliken atomic charges are the following: $+0.91$ for *K*, 1.46 for Ta and -0.79 for oxygen. These values can be compared with the results of the INDO calculations[24] [$+0.62$ (K), $+2.23$ (Ta), and -0.95 (O)]. The Wiberg index for the shortest O-Ta bond is equal to 0.57. The maximum value of the Wiberg index for a single pure covalent bond is equal to 1. So we can see that the bond O-Ta in $KTaO_3$ is rather large

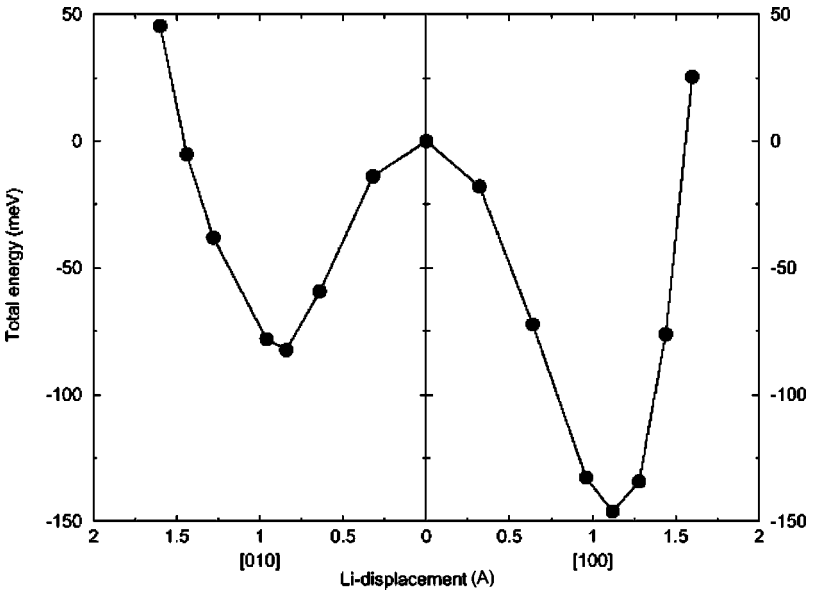

FIG. 3. Li displacements in [100] and [110] directions.

and the crystal is essentially covalent.

The band structure of KTO obtained by the INDO method appears to be practically the same as in the DFT approach because of the fitting procedure used to evaluate the INDO parameters. However the INDO calculation gave 3.6 eV for the direct gap (which is close to the experimental value). Usually the Hartee-Fock based methods overestimate the value of the optical gap, as one can see, for example, from INDO calculations[9] of KTO ($E_{\mathrm{gap}}=6.7$ eV). The accuracy of our INDO estimation is based on taking into account the polarization effects, which usually decreases the value of the optical gap.

For the system $KTaO_3$:Li the DFT calculations were made for supercells including $2\times2\times2$ primitive cells of KTO. In this supercell one K ion was replaced by Li (it corresponds to a periodical effect of substitution with a Li concentration approximately equal to 12.5%). The main features of the zone scheme appear to be the same, but at the same time the magnitude of the band gap in KTL decreases in respect to the initial perfect KTO, as will be mentioned below.

The equilibrium lattice constants a for the cubic phase of KTO and KTL were determined from the total energy calculations using DFT method. For KTO it was found that $a=3.97$ Å, which agrees excellently with the experimental value 3.998 Å (Ref. 25) and is more accurate than the 3.96 Å found in LDA calculations.[11] No changes have been found in the lattice constant for KTL 12% ($2\times2\times2$ supercell) from DFT calculations, if the relaxation of surrounding ions is neglected. We also calculated the total energy (E_t) of KTL as function of Li displacement (d) along [100] and [110] directions. These data are presented in Fig. 3.

The equilibrium off-center Li displacement along [100] was found to be 1.15 Å with an energy lowering of about 146 meV. Such a magnitude of the Li displacement agrees quite well with the NMR estimation of 1.26 Å,[26] theoretical prediction of 1.44 Å (Ref. 27) and of 1.35 Å,[28] but is sufficiently larger than the theoretical value 0.64 Å (Ref. 29) and NMR estimations of 0.86 Å.[2] Our estimation of the energy gain ($\sim$146 meV) also appeared to be larger than the theoretical value of 60 meV obtained in Refs. 24,30. Figure 4 presents the energy profile of Li^+ ions in KTL. One of the most important energy characteristics of KTL is a barrier for 90° flips of the Li^+ off-center ions, which determines, e.g., the dipole relaxation in this material. We calculated 64 meV for the barrier for such flips, which is small in respect to experimental values of about 86 meV.[28] The origin of this discrepancy is probably related to the lattice relaxation around the displaced Li^+ ion, which should be taken into consideration too, to improve the calculation accuracy.

To clear up the Li effect on the energy structure in the region of the optical absorption edge, the comparative calculations of the electronic structure of KTO and KTL were performed using the DFT method for $2\times2\times2$ supercells. For the first step only Li+ displacements for KTL were taken into account. In this case only K and Li—states lying inside of CB are considered, i.e., the energy structure and density of states appear to be identical for KTO and KTL. No local levels in the band gap of KTL were found and to inspect the Li effect in the energy structure more deeply, additional calculations with larger supercells were needed. Because DFT computations are too costly, the INDO calculation for a supercell ($4\times4\times4$) of KTO and KTL, i.e.,

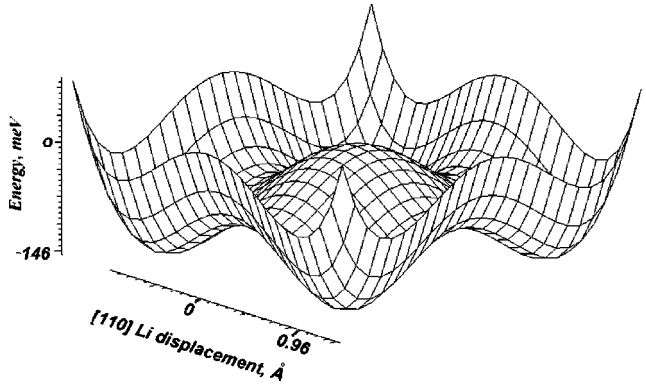

FIG. 4. Energy profile of Li+ ions in $KTaO_3$.

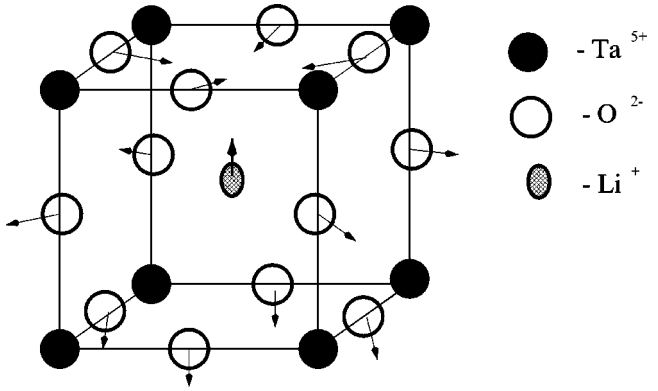

FIG. 5. Ion's displacements in $KTaO_3$:Li.

for 63 atoms of K with one substitutional Li was performed. This calculation was performed only for high symmetry points of the BZ. In this case the possibility of appearance of local states in the band gap can be inspected much more carefully. For the first step only Li displacements for INDO was taken from DFT $2\times2\times2$ calculations, but no local levels in the band gap of KTL were found either. The same result follows from INDO $2\times2\times2$ supercell calculations. However this result is not quite convincing, because oxygen displacements around the Li^+ off-center ion were not taken into account and in our experiment,[20] the indirect absorption edge for pure KTO appeared at higher energy than for KTL (3.6 eV for KTO and 3.48 eV for KTL5%). For a second step the small displacements of oxygen (see Fig. 5) ions nearby Li+ off center ions were taken into consideration too. As a result, at least for KTL1.5%, two local states appear in the bandgap at 60 and 90 meV from the top of the valence band.

Thus, new details of *ab inito* calculations of the energy structure of KTO and first calculations of the energy structure of KTL are presented. The important role of covalent bonds in KTO and KTL is shown. Our calculations, in which electron and hole polarization effects have been taken into account too, gave adequate energy structure, density of CB and VB states, magnitudes of bandgap and lattice parameters, which agree well with experimental data, without the need of additional correction parameters. Special attention is paid to the structure of Li^+ off-center impurities and the Li^+ off-center effect in the KTL energy structure. We found that the adjustment of oxygen ions around Li^+ off center ions leads to the appearance of two shallow levels in the band-gap with energy 60 and 90 meV from the top of VB. These shallow hole trap levels, whose existence at first was proposed in Ref. 4 and obtained experimentally in Refs. 31,32, can play an important role in photoconductivity and visible luminescence intensity increasing and other photoinduced properties of KTL in respect to the initial KTO crystals, in accordance with experimental results.

ACKNOWLEDGMENTS

All calulations using CASTEP code were performed at the Cavendish Laboratory (Cambridge University). We are grateful to Dr. M.C. Payne and Professor V. Heine for providing the CASTEP code and for the helpful discussions. This work is also supported by Grants No. DFG/SFB 225-C7, LN00A015 (Ministry of Education of the Czech Republic) and No. 202/00/1425 (GACR).

*Permanent address: A.F. Ioffe Institute, 194 021 St. Petersburg, Russia.

[1] M.C. Payne, M.P. Teter, D.C. Alan, T.A. Arias, and J.D. Joannopoulos, Rev. Mod. Phys. **64**, 1045 (1992).
[2] U.T. Hochli, K. Knorr, and A. Loidl, Adv. Phys. **39**, 405 (1990), and references therein.
[3] Y. Yacoby and S. Just, Solid State Commun. **15**, 715 (1974).
[4] R.S. Klein, G.E. Kugel, M.D. Glinchuk, R.O. Kuzian, and I.V. Kondakova, Phys. Rev. B **50**, 9721 (1994).
[5] U. Bianchi, W. Kleemann, and J.G. Bednorz, Ferroelectrics **157**, 165 (1994).
[6] P. Camagni, P. Galinetto, E. Giulotto, G. Samoggia, V. Trepakov, and L. Jastrabik, Ferroelectrics **239**, 225 (2000).
[7] A.V. Baryshev, S.A. Basun, V.S. Vikhnin, and V.A. Trepakov, Phys. Solid State **39**, 1941 (1997).
[8] P. Sangalli, L. Rollandi, P. Calvi, E. Giulotto, P. Camagni, and G. Samoggia, J. Korean Phys. Soc. **32**, S1104 (1998).
[9] T. Neumann, G. Borstel, C. Scharfschwerdt, and M. Neumann, Phys. Rev. B **46**, 10 623 (1992).
[10] L.F. Mattheiss, Phys. Rev. B **6**, 4718 (1972).
[11] David J. Singh, Phys. Rev. B **53**, 176 (1996).
[12] J.S. Lin, A. Qteish, M.C. Payne, and V. Heine, Phys. Rev. B **47**, 4174 (1993).
[13] L. Kleinman and D.M. Bylander, Phys. Rev. Lett. **48**, 1425 (1982).
[14] E. Clementi and C. Roetti, At. Data Nucl. Data Tables **14**, 197 (1974).
[15] J. Choisnet, R.A. Evarestov, I.I. Tupitsyn, and V. Veryazov, J. Phys. Chem. Solids **57**, 1839 (1996).
[16] K. Ohno, Theor. Chim. Acta **3**, 219 (1964).
[17] M.D. Segal, R. Shah, C.J. Pickard, and M.C. Payne, Phys. Rev. B **54**, 16 317 (1996).
[18] K.B. Wiberg, Tetrahedron **24**, 1083 (1968).
[19] I. Mayer, Int. J. Quantum Chem. **29**, 73 (1986).
[20] A. Deineka, V. Trepakov, I. Tupitsyn, L. Jastrabik, S.E. Kapphan, and P.P. Syrnikov, Radiat. Eff. Defects Solids **149**, 113 (1999).
[21] S.I. Shablaev, A.M. Danishevskii, and V.K. Subashiev, Zh. Eksp. Teor. Fiz. **86**, 2158 (1984).
[22] E. Wiesendanger, Ferroelectrics **6**, 263 (1974).
[23] *Ferroelectrics and Related Substance*, edited by K.H. Hellwege, Landolt-Bornstein: Numerical Data and Functional Relationships in Science and Technology, Vol.III/16a Oxides, (Springer-Verlag, Berlin, 1981).
[24] R.I. Eglitis, A.V. Postnikov, and G. Borstel, Phys. Rev. B **55**, 12976 (1997).
[25] G. Shirane, R. Newnham, and R. Pepisky, Phys. Rev. **96**, 581 (1954).
[26] J.J. van der Klink and F. Borsa, Phys. Rev. B **30**, 52 (1984).
[27] M.G. Staciotti and R.L. Migoni, J. Phys.: Condens. Matter **2**, 4341 (1990).

[28] J.J. Van der Klink and S.N. Khanna, Phys. Rev. B **29**, 2415 (1984).
[29] M. Exner, C.R.A. Catlow, H. Donnerberg, and O.F. Schirmer, J. Phys.: Condens. Matter **6**, 3379 (1994).
[30] A.V. Postnikov, T. Neumann, and G. Borstel, Ferroelectrics **164**, 101 (1995).
[31] P. Sangali, P. Calvi, L. Rollandi, E. Giulotto, P. Camagni, and G. Samoggia, J. Korean Phys. Soc. **32**, S811-S813 (1998).
[32] P. Galinetto, E. Giulotto, P. Sangalli, P. Camagni, and G. Samoggia, J. Phys.: Condens. Matter **11**, 1945 (1999).